Interaction of a chirally functionalised porphyrin derivative with chiral micellar aggregates. Construction of a system with stereoselective cytochrome-P450 biomimetic activity

Veronica Cantonetti,[a] Donato Monti,[a,*] Mariano Venanzi,[a] Cecilia Bombelli,[b]
Francesca Ceccacci[b] and Giovanna Mancini[b]

[a]*Dipartimento di Scienze e Tecnologie Chimiche, Università degli Studi di Roma 'Tor Vergata',
Via della Ricerca Scientifica 1, I-00133 Rome, Italy*
[b]*C.N.R. Istituto di Metodologie Chimiche—Sezione Meccanismi di Reazione, c/o Dipartimento di Chimica,
Università degli Studi di Roma 'La Sapienza', P.le Aldo Moro 5, I-00185 Rome, Italy*

Abstract—The inclusion behaviour of porphyrin derivative manganese [5-(4-(carboxyphenyl-(*N*-L-proline)))-10-15-20-tri-phenylporphyrinyl] chloride **1MnCl** in micellar aggregates of sodium *N*-dodecanoyl-L-prolinate **L-SDP** and of sodium dodecyl-sulfate **SDS** has been studied by means of several spectroscopic techniques. The catalytic activity in the epoxidation reaction of some test chiral olefins has been also investigated. Comparison with the case of the related manganese[5-(4-carboxyphenyl)-10-15-20-triphenylporphyrinyl] chloride **2MnCl**, gave evidence that suggests the presence of a chiral functionality on the periphery of porphyrin macrocycles affects their aggregation mode within the biomembrane models. This results in the modulation of their stereoselective Cytochrome P450 biomimetic activity.
© 2004 Elsevier Ltd. All rights reserved.

1. Introduction

The study of the interaction of porphyrin derivatives with membrane models, such as micelle or liposomes,[1] represents an important area of research aimed at, for example, the development of Cytochrome P450 mimics.[2] In the seminal works of Groves and co-workers,[3] for example, ad hoc tailored steroidal metalloporphyrins, were efficiently included in synthetic phospholipid vesicles, building up a catalytic system featuring a high degree of regioselectivity in the epoxidation of poly-unsaturated fatty acids or diolefinic sterols. Nolte and co-workers developed a P450 supramolecular mimic by assembling a manganese porphyrin derivative and an amphiphilic rhodium(III) complex within a bilayer of surfactants.[4] This bimetallic system has been shown to catalyse the $O_2/HCOO^-$ promoted oxidation of various olefin derivatives, with very high turnover numbers. Along these line, we carried out some studies aimed at the construction of Cytochrome P450 mimics, based on

the incorporation of amphiphilic porphyrin derivatives within micellar aggregates, in the presence of oxygen atom donors such as H_2O_2 or $NaClO$.[5]

One of the most important factors influencing the activity of the mentioned systems, is the specificity of the interactions between the included porphyrins and the aggregates. These interactions can be effectively modulated by structural changes of the involved species, such as, for example, the charge of functional groups on the periphery of porphyrin macrocycles,[6a,b,c] the pH of the aqueous medium,[6d] or the nature and the morphology of surfactant aggregates.[7] We recently reported that the presence of a chiral functionality on the periphery of a porphyrin derivative, resulted in a selective interaction with the chiral micellar aggregates, influencing the aggregation state of any included tetrapyrrole macrocycles.[8a]

Herein we report on the results obtained in the spectroscopic investigation of the interaction of a proline-functionalised porphyrin derivative, **1MnCl**, with micellar aggregates formed by either sodium dodecyl sulfate **SDS** or sodium *N*-dodecanoyl-L-prolinate

* Corresponding author. Tel.: +39-06-7259-4328; fax: +39-06-7259-4738; e-mail: monti@stc.uniroma2.it
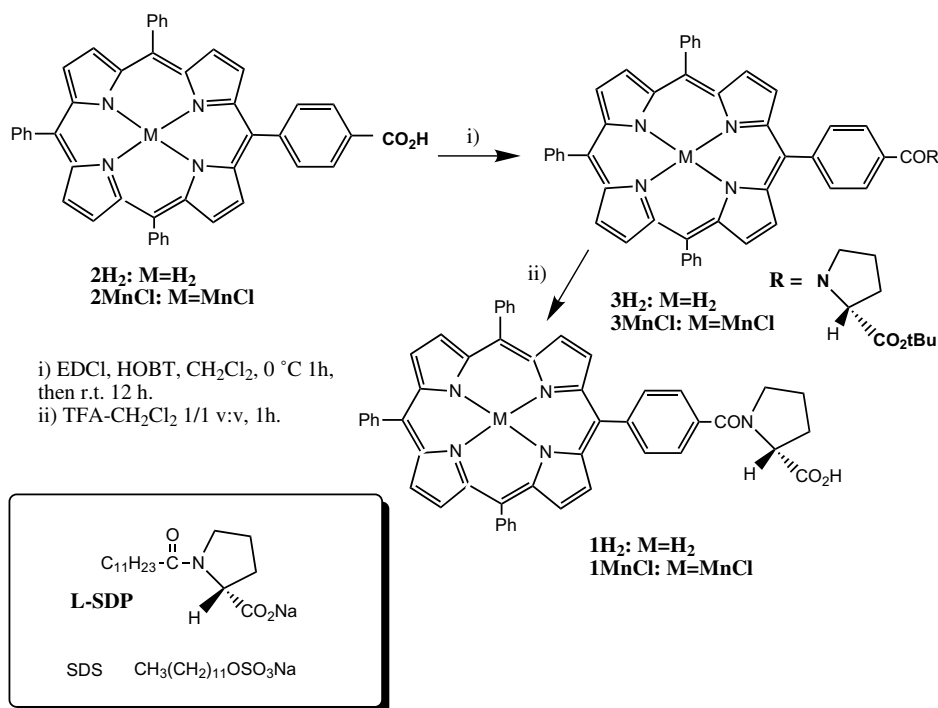
Scheme 1. Porphyrin derivatives and surfactants employed in the spectroscopic studies.

L-SDP (Scheme 1). Furthermore, their P450 biomimetic activity, in terms of regio- and stereoselectivity, was evaluated in the epoxidation reaction of (*R*)-(+)-limonene carried out in aqueous solution of **L-SDP** or in **SDS**. Comparison to that of a *p*-carboxyphenyl-porphyrin derivative **2MnCl**,[5b] a related macrocycle lacking the chiral appended functionality, gave important information on the mode of interaction and location of the porphyrin solutes as a function of their structural features, and consequently, on the effect on their reactivity.

2. Results and discussion

2.1. Preparation and spectroscopic studies

L-SDP surfactant was prepared as previously reported.[9] Porphyrin derivatives **2H$_2$** and **2MnCl** were prepared according to earlier reported procedures.[5b] Porphyrin **1H$_2$** and **1MnCl** were prepared by following the protocol outlined in Scheme 1 and have been characterised by UV–vis absorption and fluorescence spectroscopy, ^{1}H NMR and FAB-MS.

EDCl-HOBT coupling[10] of carboxy-porphyrin derivative **2H$_2$** with L-proline-*t*-butyl ester gave, after work-up and column chromatography, intermediate **3H$_2$**. Deprotection of the acidic function was subsequently accomplished by straightforward hydrolysis under acidic conditions,[11] to give the target **1H$_2$** in a satisfactory 48% overall yield, after work-up and crystallisation.

An analogous procedure carried out on **2MnCl** gave the **1MnCl** counterpart in 35% yield. Attempts to obtain the
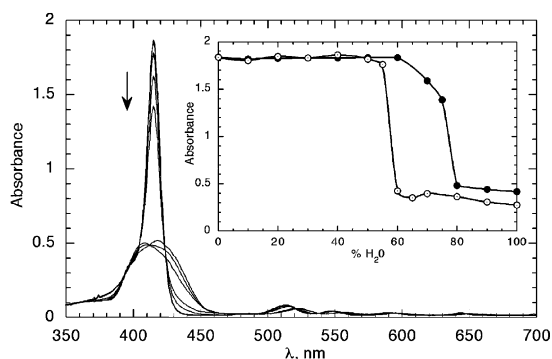
latter porphyrin derivative by direct MnCl$_2$/DMF metallation of **1H$_2$** were unsuccessful. Only traces of the desired product, along with some **2MnCl** (i.e., loss of L-proline functionality), could be recovered. Porphyrins **1MnCl** and **2MnCl** show the typical intense ligand to metal charge transfer band (LMCT) at ca. 470 nm in chlorinated solvents. The relative λ_{max} showed some dependence on the polarity of the medium (Table 1), being hypsochromically shifted (5–10 nm) in more polar solvents. This can be ascribed to the axial coordination of solvent molecules.[12] Two, nearly collapsing Q bands are also featured, as expected, in the 500–650 nm region of the spectra.

Porphyrins **1H$_2$**, **2H$_2$** and **1MnCl**, were readily soluble in chlorinated solvents, THF, ethanol or an ethanol/water mixture, but insoluble in pure water. Selected UV–vis spectroscopic data are reported in Table 1. The UV–vis spectra of **1H$_2$**, for example, feature the four visible Q-bands in the range 510–650 nm with a typical Soret band in the range 414–419 nm, dependent on the polarity of the solvent. The CD spectrum of the **1H$_2$** ethanol solution (Fig. S1; ESI) featured the typical dichroic band of the L-proline residue centred at 230 nm $\{[\theta] = 5500 \deg cm^2 dmol^{-1}$, at λ 230 nm$\}$. These porphyrin derivatives were further characterised by studying their self-aggregation behaviour, at μM concentrations, in ethanol/water mixtures. The results are reported graphically in Figure 1.
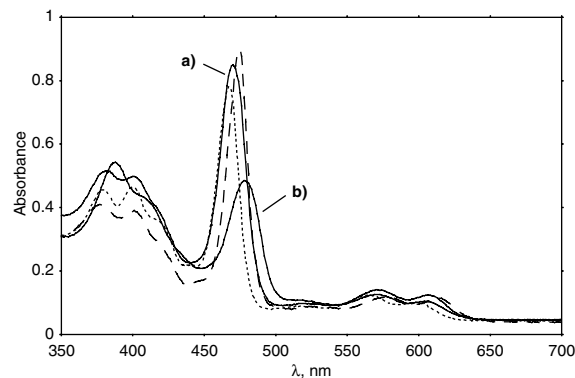
Interesting differences were found for **1H$_2$** and **2H$_2$**: As far as **1H$_2$** is concerned, a strong hypochromic effect and a broadening of the absorption bands were observed (λ 430 nm, fwhm >60 nm) when increasing the proportion of water. The absorbance maxima were concomitantly

Table 1. Spectroscopic data of porphyrin derivatives in different media[a]

Porphyrin	Medium	λ_{max}, nm (log ε)
1H$_2$	CHCl$_3$	419(5.1) 514(3.8) 546(3.8) 586(3.7) 642(3.5)
	EtOH	414(4.9) 514(3.7) 546(3.8) 585(3.5) 643(3.4)
	SDS	418(4.8) 513(3.9) 544(3.4) 585(3.3) 642(3.2)
	L-SDP	419(5.0) 513(4.0) 546(3.6) 589(3.4) 642(3.2)
2H$_2$	CHCl$_3$	419(5.2) 515(3.9) 550(3.8) 590(3.6) 645(3.3)
	SDS	418(4.8) 515(3.9) 549(3.3) 587(3.3) 643(3.2)
	L-SDP	417(4.6) 516(3.7) 550(3.2) 590(3.0) 645(2.9)
1MnCl	CHCl$_3$	378(4.6) 403(4.6) 425(4.4) 466(4.8) 561(3.9) 598(3.8)
	EtOH	379(4.5) 400(4.7) 420(4.3) 474(4.8) 561(3.8) 613(3.8)
	SDS	379(4.3) 401(4.8) 420(4.2) 471(4.5) 572(3.7) 607(3.4)
	L-SDP	379(4.5) 400(4.7) 420(4.3) 470(4.6) 572(3.7) 606(3.6)
2MnCl	CHCl$_3$[b]	377(4.6) 403(4.4) 469(5.1) 582(3.8) 618(3.7)
	EtOH	379(4.5) 400(4.7) 467(5.0) 567(4.0) 601(3.5)
	SDS	380(4.0) 401(3.9) 473(4.2) 570(3.4) 610(3.2)
	L-SDP[b]	381(4.1) 400(4.1) 472(4.3) 570(3.6) 609(3.5)

[a] [Porphyrin] $= 3 \times 10^{-6}$ M. $T = 25\,°C$. [Surfactants] $= 0.10$ M.
[b] From Ref. 5b.

Figure 2. UV–vis spectra of **1MnCl** (1.0×10^{-5} M) in different media: (a) **L-SDP** 0.10 M; (b) **SDS** 0.10 M; (dashed) CHCl$_3$; (dotted) EtOH.

more regular porphyrin to porphyrin interaction. The aggregation process is governed by specific chiral interactions that results, as recently demonstrated,[8] in the formation of chiral suprastructures.

Analogous studies on the behaviour of **1MnCl** in various media were also carried out with the results graphically reported in Figure 2. The position of the absorption maxima of the Soret, Q and LMCT bands depended on the polarity of the solvent, with it being hypsochromically shifted in more polar or protic media, as a consequence of metal co-ordination and the aggregation state of the chromophore.

The studies of the inclusion in micellar solutions provided interesting informations on their own mode of binding. Micellar solutions are constituted by 0.1 M surfactant aqueous solutions, well above their critical micelle concentration.[14] UV–vis spectra of **1MnCl** in **L-SDP** featured the expected bands with the λ_{max} somewhat red-shifted (up to 5 nm) with respect to that observed in ethanol. This finding suggests an inclusion of the chromophore in a hydrocarbon like region of the micelle. Moreover, the sharpness of the LMCT band indicates that the chromophore is included in the non-aggregated form. On the contrary the inclusion of **1MnCl** in **SDS** occurs with consistent degree of aggregation, as indicated by the broadening and hypochromicity of the relative Soret and LMCT bands.[15] These results gave evidence of the role of the porphyrin-appended functionalities on the selectivity of the solute-micelle molecular recognition processes. In the case of the porphyrin **1MnCl**, the presence of the L-proline moiety drives a more efficient recognition process within the chiral micelle.

CD spectroscopy studies on the inclusion of **1MnCl** within different micellar phases gave more insight on the interaction of the macrocycle with the surfactant aggregates. The inclusion of **1MnCl** in the **L-SDP** micelle, for example, resulted in a bisignate, negative band centred at ca. 450 nm (LMCT feature, $[\theta]_{max} \pm 4000$ deg cm^2 dmol^{-1}; Fig. 3), as a result of the Induced Circular Dichroism (ICD) by the chiral biomembrane model.[16] Some experimental evidence, such as the independence of the molar ellipticity of the

Figure 1. UV–vis spectra of **1H$_2$** (1.0×10^{-5} M) in ethanol/water mixtures at increasing water proportion. Uppermost curve: 0% H$_2$O; lowermost curve: 95% H$_2$O. Inset: aggregation curves of **1H$_2$** (●) and **2H$_2$** (○) derivatives at the corresponding water/ethanol mixtures.

shifted at somewhat longer wavelength. The corresponding absorbance versus solvent composition profile showed a sharp inflection point at water proportion $\geqslant 75\%$. This indicated the formation of porphyrin, probably J-type, aggregates[13] by a controlled self-assembling process, as evidenced by the presence of isosbestic points at 396 and 520 nm. In the case of the carboxylic derivatives **2H$_2$** the aggregation occurred at a significantly lower water proportion (i.e., $\geqslant 55\%$; Fig. 1, inset). Also in this case, the hypochromicity and bathochromic shift of the absorption maxima suggested the occurrence of aggregation. However, the absence of any clearly defined isosbestic points (Fig. S2; ESI) testifies the formation of different species of porphyrin aggregates. This finding indicates that the nature of the appended functionality influences the self-recognition process during the porphyrin aggregation event. Evidently, the presence of the L-proline residue steers a
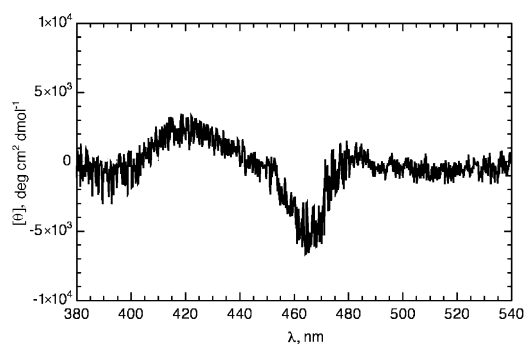
Figure 3. CD spectra of **1MnCl** (8.5×10^{-6} M) in **L-SDP** 0.10 M.

porphyrin concentration (not shown) within the concentration range examined, and the sharpness of the relative Soret band (UV–vis), ruled out the formation of porphyrin aggregated species (i.e., π–π stacked). Ethanol solutions of **1H₂** were CD silent in the 350–500 nm range (i.e., in the porphyrin Soret and LMCT region) even in the presence of **L-SPD** (0.1 M). The fact that in ethanol (i.e., non-aggregating conditions) we did not observe any ICD, implies that is the stereochemical information possessed by the surfactant aggregates, that must be effectively read-out by the included macrocycles upon noncovalent, specific, interactions. Interestingly, a EtOH/H_2O (20/80, v/v) solution of **1H₂** featured a coupled CD band, red-shifted at 480 nm, with opposite (i.e., positive) sign with respect to that performed in **L-SDP**. Moreover, the intensity, higher than that observed in **L-SDP** ($[\theta]_{max} \pm 6000 \, \text{deg cm}^2 \, \text{dmol}^{-1}$; Fig. 4), and the shape, were largely dependent on the porphyrin concentration.

This finding, along with the presence of some broadening of the Soret band (UV–vis), implies the formation of porphyrin chiral aggregates with the L-proline appended residues driving the helical sense of the self-assembling process.[17] Analogous behaviour was observed upon inclusion of **1MnCl** in **SDS** 0.1 M. This should corroborate the hypothesis, as already evidenced by UV–vis spectroscopic studies, that the inclusion of **1H₂** in **SDS** occurs with a consistent degree of self-aggregation (see Fig. 2), towards a chiral structure, driven by the L-proline functionality. On the other hand, the achiral
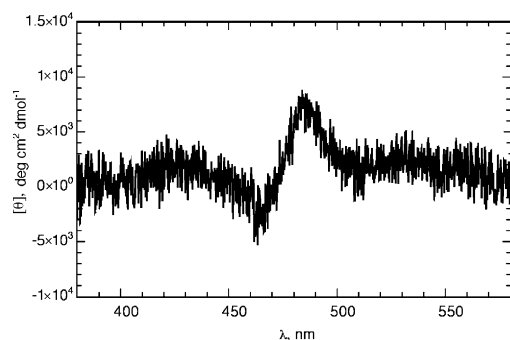
2MnCl derivative became CD silent once included in **L-SDP** micelle in either monomeric form or in aggregative conditions. This finding could be the consequence of the inclusion of the macrocycle in a nonchiral region of the micelle, or of scarcely specific interactions between the porphyrin macrocycle and the aggregates. This behaviour was also encountered in the case of parent free-base macrocycles, indicating that the presence of the central metal atom does not heavily influence the interaction with the surfactant aggregates.

Fluorescence spectroscopy studies on the Mn(III) derivatives, could not be carried out as the presence of the heavy metal atom precluded the acquisition of fluorescence signals.[12] However, quenching fluorescence experiments, were carried out on the parent **1H₂/L-SDP** system in order to acquire information on the localisation of the macrocycles within the biomembrane models, with the assumption that the absence of the central metal atom would not dramatically affect the topology of inclusion. The use of 'depth-dependent' lipophylic quenchers[18] such as 2-bromooctanoic acid and 16-bromo-hexadecanoic acid, **C2-Br**, and **C16-Br**, respectively, provided some information on the location of **1H₂** in the chiral micellar aggregates. The different effect of the probes could imply a preferential location of the porphyrin solute within the micelle.

In fact, the fluorescence of the **1H₂** was quite affected by **C16-Br** whereas it could not be quenched by **C2-Br** (Fig. 5), indicating a location of the macrocycle in an internal, hydrophobic region, of the surfactant aggregate. From the corresponding plot, a Stern–Volmer quenching constant of K_{SV} 15 M^{-1} can be estimated. The value is in line with those commonly observed in the case of static quenching with a bromide ion.[18d]

The cytochrome P450 biomimetic epoxidation[2a] ability of **1MnCl** was tested in either chiral **L-SPD**, or in **SDS** 0.1 M aqueous solutions, by following a protocol reported in the Experimental section, and outlined in Scheme 2. The results have been compared to those obtained in the case of the achiral **2MnCl**, and are summarised in Table 2. (R)-(+)-limonene **1** was chosen
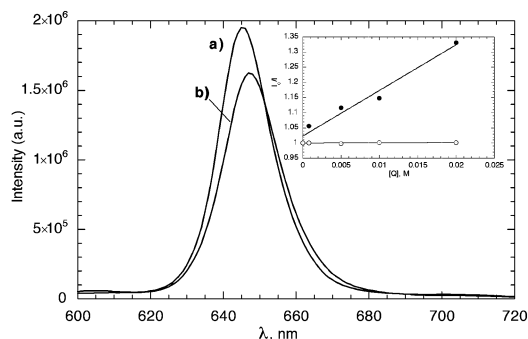

Figure 4. CD spectra of **1MnCl** (8.5×10^{-6} M) in 90% (v/v) water/ethanol mixture.
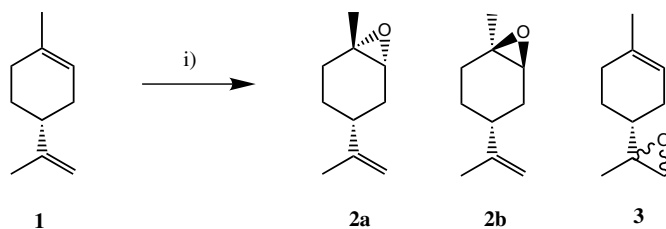

Figure 5. Fluorescence emission spectra of **1H₂** (8.5×10^{-6} M) in (a) **L-SPD** 0.10 M, and (b) **SDS** 0.10 M. Inset: Stern–Volmer plot of the fluorescence quantum yield of **1H₂** (8.5×10^{-6} M) in **L-SDP** 0.10 M, at varying concentrations of 16-bromohexadecanoyc acid (●), and 2-bromooctanoic acid (○).

Scheme 2. Scheme of epoxidation reaction in various media. (i) [limonene] = 0.02 M; [catalyst] = 3×10^{-3} M; [imidazole] = 0.10 M; [H$_2$O$_2$] = 0.06 M; [surfactant] = 0.10 M; rt, 10 min.

Table 2. Epoxidation of *R*-(+)-limonene in different media by H$_2$O$_2$[a]

Entry	Catalyst	Medium	Epoxide (%)[b]	De[c]
1	**1MnCl**	**L-SDP**	>95	42
2	**1MnCl**	**SDS**	55	<5
3	**1MnCl**	EtOH/H$_2$O[d]	15[e]	0
4	**2MnCl**	**L-SDP**	60	10[f]
5	**2MnCl**	**SDS**	15	0
6	**2MnCl**	EtOH/H$_2$O[d]	15[e]	0

[a] [Limonene] = 0.02 M; [catalyst] = 3.0×10^{-3} M; [imidazole] = 0.10 M; [H$_2$O$_2$] = 0.6 M; [surfactant] = 0.10 M.
[b] Percentage referred to starting olefin.
[c] De is the diastereomeric excess of the 1,2-epoxide isomers (*syn* vs *anti*).
[d] Ethanol/water 80:20, v/v solvent mixture.
[e] Regioselectivity *endo/exo* ca. 1/2.
[f] From Ref. 5b.

as a test substrate, as it has (i) a good solubility in **L-SPD**,[5b] (ii) two different double bonds, namely an endocyclic and an external one and (iii) a stereogenic centre. The results obtained provide useful information on the intimate structure of the whole (i.e., micelle/substrate/catalyst) system. The reactions occurred smoothly at room temperature, with H$_2$O$_2$ as oxidant, in the presence of an excess amount of imidazole as co-catalyst. The reaction when carried out in homogeneous medium (EtOH/H$_2$O, 80:20 v/v) resulted in a lower degree of conversion, with respect to that already carried out in micellar phases.

This could be inferred to the onset of catalyst deactivation paths, such as for example the formation of porphyrin μ-oxo derivatives, promoted by porphyrin self-association[2] or catalyst bleaching, that are prevented in micellar phases. A poorer degree of regioselectivity was also seen. Moreover, the lack of diastereoselectivity presented by the chiral functionalised **1MnCl**, analogous to that observed for the achiral **2MnCl**, prove that the mere presence of a stereogenic centre on the periphery of the macrocycle does not affect the stereochemical course of the reaction (entries 3 and 6, Table 2). Reactions carried out in micellar phases proceeded with higher yield and towards the almost exclusive (>95% of regioselectivity) attack on the internal double bond (i.e., formation of 1,2-epoxides **2a** and **2b**), being the external epoxides **3** (attack on the 8,9 double bond) formed in very low amounts. This reflects the rigid geometrical constraints of the substrate inside the micellar aggregates, resulting in a preferential exposition of one of the double bonds to the catalytic metal centre. The decreased reactivity observed in the case of the reaction carried out in **SDS**, should be

inferred to the aggregation of the catalyst in this micellar system. It is noteworthy that when the reaction was carried out in **L-SDP** it proceeded with an appreciable degree of diastereoselectivity towards the preferential formation of the *syn*-epoxide **2a** over the *anti*-diastereoisomer **2b**.[19] This result, although not exceptional from a synthetic point of view, showed an increased stereoselectivity featured by the **1MnCl/L-SPD** system (de ca. 40, entry 1; Table 2) compared to the other catalytic systems, namely **1MnCl/SDS** (de ca. 5, entry 2; Table 2) and **2MnCl/L-SDP** (de ca. 10, entry 4; Table 2). As expected, the reaction carried out under homogeneous conditions resulted in no diastereomeric excess. All these findings suggest that the presence of the asymmetric environment of the chiral micellar aggregates influences the stereoselectivity of the reaction; it should be noted that this can not be the only factor affecting the observed chiral induction. The selective interaction of the catalyst with the biomembrane model, as concomitantly evidenced by the spectroscopic studies, must also play a decisive role on the observed phenomenon. Moreover, the results obtained indicate, according to the fluorescence quenching experiments, that the catalytic active site (i.e., the metal centre) should be located in the inner region of the micelle, that is within the hydrophobic tail of the surfactants (quenching studies). It is known that a reaction occurring in a surfacial area of the micelle aggregates, usually yields a lower extent of stereoselectivity.[5b] This has been reported, for example, in some Rh(I)-catalysed asymmetric hydrogenation reaction[20] carried out in similar L-proline amphiphilised derivatives, in which the small enantiomeric excess observed has been interpreted as the consequence of the location of the catalyst in a surfacial area (i.e., the palisade layer) of the micelles. In our case,

the results can be interpreted on the basis of the formation of an internal chiral pocket, steered by the interaction of the porphyrin functionality with the chiral surfactant polar head group.[21] Although it is known[22] that aggregates formed by chiral surfactants may yield chiral recognition, the case herein, in our opinion, is quite novel. The chirality featured by the involved porphyrin macrocycles (demonstrated by both CD and reactivity experiments) is transmitted by the chiral head groups to an internal region of the micelle (i.e., hydrocarbon region) that, otherwise, would have been expected to feature, at least in principle, a low extent of organisation.

3. Conclusions

The spectroscopic studies on the interaction of chirally functionalised porphyrin derivatives with chiral micelle aggregates point out the important role played by the presence of the appended group on their inclusion behaviour. The results obtained in CD and reactivity experiments suggest that chiral recognition takes place in the hydrophobic region of the aggregates where a chiral environment is transmitted by the polar head groups to the hydrophobic chains. These amino acid-functionalised porphyrins[23] are of particular interest for the development of hemoprotein models[24] or multi-haem protein mimics for redox catalysis and energy conversion in respiratory and photosynthetic electron transfer.[25]

4. Experimental section

4.1. Instrumentation

UV–vis spectra were performed on a Perkin Elmer λ18 Spectrophotometer equipped with a thermostated cell holder.

CD spectra were performed on a JASCO J-600, equipped with a thermostated cell holder, and purged with ultra-pure nitrogen gas.

Steady-state fluorescence spectra were recorded on a SPEX Fluoromax Spectrofluorometer, operating in single photon counting (SPC) mode. Nanosecond decays were measured by a CD900, SPC lifetime apparatus from Edinburgh Instruments.

GC analyses were performed on a Carlo Erba HRGC equipped with a Supelco SPB-35 capillary column. GC–MS runs have been performed on a Varian 3400 matched to a mass selective Hewlett–Packard HP-5970 detector.

4.2. Materials

Chemicals (Aldrich, Merck or Fluka) were of the highest grade available and used without further purification. Silica gel 60 (70–230 mesh) was used for column chro-matography. Solvents were dried, distilled and degassed prior to use by using standard procedures.[26] Solvents employed in the spectroscopic studies are of spectroscopic grade and used as received. **SDS** (Fluka) was used as received. Aqueous solutions of the surfactants were found to be fluorescence free and were used as such.

4.3. UV–vis and CD spectroscopic studies

Incorporation of the substrates in micellar phases were accomplished by injection of the required amount of porphyrin stock solution (1–5 mM ethanol solution) in 0.10 M doubly distilled water solution of surfactants. The resulting solutions were incubated at 35 °C for 30 min. The clear solutions obtained (final porphyrin concentration within the range 1×10^{-7}–1×10^{-5} M) were found to be stable in the dark at room temperature, with no significant alteration (UV–vis check of the band intensities) or precipitation observed after several months of storage.

4.4. Fluorescence spectroscopy experiments

All fluorescence experiments were carried out in quartz cells, using freshly prepared solutions, thermostated at 25 °C. Quenching experiments were carried out by measuring the fluorescence of the porphyrin (typically 5×10^{-6} M) in 0.10 M surfactant solution containing different concentration of quenchers (0–0.025 M). The solutions were prepared by co-dissolving in a 2 mL volumetric flask the required amount of quencher, surfactant and porphyrin into the minimum amount of absolute ethanol. The solvent was evaporated (gentle warming under a nitrogen stream) and the residue dissolved in 2 mL of distilled water (Millipore grade). This procedure ensured a constant concentration of the porphyrin fluorophore throughout the titration experiment. Spectra were acquired after 15 min of incubation at 35 °C.

4.5. Preparation of porphyrin derivatives

All the reactions were carried out under an inert atmosphere. The protocol for the synthesis of **2H₂** and **2MnCl**, outlined in Scheme 1, has previously been reported.[5b]

4.6. 5-[4-(Carboxyphenyl-(*N*-ʟ-proline *t*-butyl ester))]-10-15-20-triphenylporphyrin 3H₂

To a stirred solution of 0.14 g of **2H₂** (0.211 mmol) in 25 mL of CH₂Cl₂ kept at 0 °C, 0.041 g of 1-[3-(dimethyl-amino)propyl]-3-ethylcarbodiimide hydrochloride (EDCl, 0.211 mmol) and 0.029 g of 1-hydroxy-1*H*-benzotriazole (HOBT, 0.211 mmol were added). The solution was stirred, at 0 °C for 1 h, then an excess of ʟ-proline *t*-butyl ester (0.11 g; 0.633 mmol) added. The reaction mixture was stirred at room temperature overnight. The

solvent was then removed under reduced pressure and the residue dissolved in 100 mL of chloroform and extracted with brine (3 × 100 mL). The organic layer was dried over Na_2SO_4 and the solvent evaporated to give 125 mg of pure **3H₂** (TLC) as purple solid. Further purification (SiO_2 chromatography, $CHCl_3/CH_3OH$ 9:1 v/v as eluant) gave 105 mg of **3H₂** (0.130 mmol; 61% yield) as bright purple crystals. UV–vis ($CHCl_3$): λ_{max} (log ε) 419 (5.1), 514 (3.8), 546 (3.6), 586 (3.7), 645 (3.2). FAB-MS (NBA), m/e: 811 $[M-H]^+$.

4.7. 5-[4-(Carboxyphenyl-(*N*-ʟ-proline))]-10-15-20-triphenylporphyrin 1H₂

In a 50 mL round bottomed flask, 100 mg of **3H₂** (0.123 mmol) were dissolved in 50 mL of CH_2Cl_2/trifluoroacetic acid (1:1 v/v). The reaction mixture was stirred, at room temperature, for 1 h. The solvent was then evaporated under reduced pressure and the greenish residue dissolved in 50 mL of chloroform and washed with 50 mL of a saturated $NaHCO_3$ aqueous solution. The organic layer was dried over Na_2SO_4, evaporated and the solid crystallised ($CHCl_3$/hexane) to give 75 mg (0.10 mmol; 80% yield) of purple crystals of pure **1H₂**. UV–vis ($CHCl_3$): λ_{max} (log) 419 (5.1), 514 (3.8), 546 (3.8), 586 (3.7), 642 (3.5). FAB-MS (NBA), m/e: 756 $[M+H]^+$. ¹H NMR ($CDCl_3$), δ: 9.1–8.5 (br s, 8H, pyrrole β-Hs), 8.25 (d, $J = 8.2$ Hz, 2H, 3′-C_6H_4OR), 8.15 (d, $J = 8.2$ Hz, 2H, 2′-C_6H_4OR), 4.7–4.5 (m, 1H, proline α-H), 4.8–3.7 (m-2H, proline δ-H), 2.5–1.9 (m, proline, γ, β-Hs), −2.79 (br s, 2H, pyrrole NH) ppm.

4.8. Manganese[5-(4-(carboxyphenyl-(*N*-ʟ-proline *t*-butyl ester)))-10-15-20-triphenylporphyrinyl] chloride 3MnCl

The preparation of **3MnCl** was accomplished by following the procedure reported for **3H₂**. Starting from 0.190 g of **2MnCl** (0.270 mmol), 0.039 g of HOBT (0.028 mmol) and 0.054 g of EDCl (0.028 mmol), 0.150 g of **3MnCl** (0.160 mmol; 45% yield) was obtained after work-up and column chromatography (SiO_2, $CHCl_3$/CH_3OH 1:1 v/v as eluant). UV–vis ($CHCl_3$): λ_{max} (log ε) 376 (4.6), 425 (4.4), 468 (4.8), 561 (3.9), 598 (3.8). FAB-MS (NBA), m/e: 865 $[M-Cl]^+$.

4.9. Manganese[5-(4-(carboxyphenyl-(*N*-ʟ-proline)))-10-15-20-triphenylporphyrinyl] chloride 1MnCl

The preparation of **1MnCl** was accomplished by following the procedure reported for **1H₂**. Starting from 0.10 g of **3MnCl** (0.110 mmol), 0.070 g of **1MnCl** was obtained (0.086 mmol; 78% yield) after work-up and crystallisation ($CHCl_3$/hexane). UV–vis ($CHCl_3$): λ_{max} (log ε) 378 (4.6), 403 (4.6), 425 (4.4), 466 (4.8), 561 (3.9), 598 (3.8). FAB-MS (NBA), m/e: 809 $[M-Cl]^+$.

4.10. Epoxidation reactions

The solutions for the epoxidation experiments were prepared, in a 3 mL vial equipped with magnetic stirring

apparatus, by co-dissolving the required amount of porphyrin catalysts **1MnCl** or **2MnCl**, and imidazole in 400 μL of dichloromethane. The resulting solution was briefly sonicated to homogeneity and the solvent then removed by gentle warming with the aid of an argon stream. The appropriate surfactant solution (2 mL) containing the required amount of olefin was then added and the resulting mixture stirred and sonicated until dissolution. The reaction mixture was incubated at 35 °C for 15 min and then cooled to 25 °C. Aliquots of 1.0 M H_2O_2 aqueous solution were added and the resulting mixture (final concentration of 0.6 M) vigorously stirred for 10 min. This reaction time allowed us to observe the differences between the catalytic systems: However by prolonging the reaction time, some decomposition of the epoxides (i.e., ring opening) can occur. An internal standard (*n*-decane or *n*-dodecane) was then added and an aliquot (200 μL) of the reaction mixture then taken, quenched with methanol (100 μL) (in order to disrupt the micellar aggregates) filtered from the eventually precipitated salts and extracted with petroleum ether. The organic phase was analysed by GC and GC–MS. Runs were triplicated and were reproducible within 5%. The reaction products were characterised by comparisons (GC and GC–MS) with authentic samples. As far as the reactions in aqueous solvent mixture were concerned, the oxidant was added to a 2 mL solution of catalyst, imidazole and olefin, in the appropriate molar ratio. The reaction mixture was then extracted (petroleum ether) and analysed as described above.

References and notes

1. Bunton, C. A.; Savelli, G. *Adv. Phys. Org. Chem.* **1986**, *22*, 213–309.
2. (a) Ortiz de Montellano, P. R. *Cytochrome P-450: Structure, Mechanism and Biochemistry*, 2nd ed.; Plenum: New York, 1995; For recent surveys on porphyrin-catalysed oxidations see: (b) Meunier, B.; Robert, A.; Pratviel, G.; Bernadou, J. In *The Porphyrin Handbook*; Kadish, K. M., Smith, K. M., Guilard, R., Eds.; Academic: New York, 2000; Vol. 4, p 119; (c) Suslik, K. S. In *The Porphyrin Handbook*; Kadish, K. M., Smith, K. M., Guilard, R., Eds.; Academic: New York, 2000; Vol. 4, p 41.
3. (a) Groves, J. T.; Neumann, R. *J. Am. Chem. Soc.* **1987**, *109*, 5045–5047; (b) Groves, J. T.; Neumann, R. *J. Am. Chem. Soc.* **1989**, *111*, 2900–2909; (c) Groves, J. T.; Fate, G. D.; Lahiri, J. *J. Am. Chem. Soc.* **1994**, *116*, 5477–5478.
4. (a) Feiters, M. C.; Rowan, A. E.; Nolte, R. J. M. *Chem. Soc. Rev.* **2000**, *29*, 375–384; (b) Schenning, A. P. H. J.; Lutje Spelberg, J. H.; Hubert, D. H. W.; Feiters, M. C.; Nolte, R. J. M. *Chem. Eur. J.* **1998**, *4*, 871–880;

(c) Schenning, A. P. H. J.; Hubert, D. H. W.; van Esch, J. H.; Feiters, M. C.; Nolte, R. J. M. *Angew. Chem., Int. Ed. Engl.* **1994**, *33*, 2468–2470; (d) van Esch, J. H.; Roks, M. F. M.; Nolte, R. J. M. *J. Am. Chem. Soc.* **1986**, *108*, 6093–6094.

5. (a) Monti, D.; Tagliatesta, P.; Mancini, G.; Boschi, T. *Angew. Chem., Int. Ed.* **1998**, *37*, 1131–1133; (b) Borocci, S.; Marotti, F.; Mancini, G.; Monti, D.; Pastorini, A. *Langmuir* **2001**, *17*, 7198–7203; (c) Monti, D.; Pastorini, A.; Mancini, G.; Borocci, S.; Tagliatesta, P. *J. Mol. Catal. A* **2002**, *179*, 125–131.

6. (a) Schenning, A. P. H. J.; Hubert, D. H. W.; Feiters, M. C.; Nolte, R. J. M. *Langmuir* **1996**, *12*, 1572–1577; (b) Schell, C.; Hombrecher, H. K. *Chem. Eur. J.* **1999**, *5*, 587–598; (c) Vermathen, M.; Luie, E. A.; Chodosh, A. B.; Ried, S.; Simonis, U. *Langmuir* **2000**, *16*, 210–221; (d) Zhang, Y.-H.; Guo, L.; Ma, C.; Li, Q.-S. *Phys. Chem. Chem. Phys.* **2001**, *3*, 583–587.

7. (a) Ricchelli, F. J. *Photochem. Photobiol. B: Biol.* **1995**, *29*, 109–118; (b) Ricchelli, F.; Gobbo, S. J. *Photochem. Photobiol. B: Biol.* **1995**, *29*, 65–70, and references cited therein; (c) Monti, D.; Venanzi, M.; Cantonetti, V.; Borocci, S.; Mancini, G. *J. Chem. Soc., Chem. Commun.* **2002**, 774–775.

8. (a) Monti, D.; Cantonetti, V.; Venanzi, M.; Ceccacci, F.; Bombelli, C.; Mancini, G. *J. Chem. Soc., Chem. Commun.* **2004**, 972–973; For some recent, important examples, on the interaction of porphyrin derivatives with DNAs or other chiral polymeric matrices see: (b) Pasternack, R. F.; Gibbs, E. J.; Bruzewicz, D.; Stewart, D.; Engstrom, K. S. *J. Am. Chem. Soc.* **2002**, *124*, 3533–3539; (c) Pasternack, R. F.; Ewen, S.; Rao, A.; Meyer, A. S.; Freedman, M. A.; Collings, P. J.; Frey, S. L.; Ranen, M. C.; de Paula, J. C. *Inorg. Chim. Acta* **2001**, *317*, 59–71; (d) Purrello, R.; Monsú Scolaro, L.; Bellacchio, E.; Guerrieri, S.; Romeo, A. *Inorg. Chem.* **1998**, *37*, 3647–3648; (e) Bellacchio, E.; Lauceri, R.; Gurrieri, S.; Monsù Scolaro, L.; Romeo, A.; Purrello, R. *J. Am. Chem. Soc.* **1998**, *120*, 12353–12354; (f) Purrello, R.; Bellacchio, E.; Guerrieri, S.; Lauceri, R.; Raudino, A.; Monsù Scolaro, L.; Santoro, A. M. *J. Phys. Chem. B* **1998**, *102*, 8852–8857; (g) Pasternack, R. F.; Gurrieri, S.; Lauceri, R.; Purrello, R. *Inorg. Chim. Acta* **1996**, *246*, 7–12; Polymer-anchored porphyrin nanorods with helical structure have been recently reported: (h) de Witte, P. A. J.; Castriciano, M.; Cornelissen, J. J. L. M.; Monsù Scolaro, L.; Nolte, R. J. M.; Rowan, A. E. *Chem. Eur. J.* **2003**, *9*, 1775–1781; For recent reports on the chiral-symmetry-breaking in the self-association of achiral porphyrin derivatives see: (i) Rubires, R.; Ferrera, J.-A.; Ribó, J. M. *Chem. Eur. J.* **2001**, *7*, 436–446; (j) Borovkov, V. V.; Harada, T.; Hembury, G. A.; Inoue, Y.; Kuroda, R. *Angew. Chem., Int. Ed.* **2003**, *42*, 1746–1749; For an example of chiral memory in templated-imprinted chiral porphyrin aggregates: (k) Lauceri, R.; Raudino, A.; Monsù Scolaro, L.; Micali, R.; Purrello, R. *J. Am. Chem. Soc.* **2002**, *124*, 894–895.

9. (a) Jungermann, E.; Gerecht, J. F.; Krems, I. J. *J. Am. Chem. Soc.* **1956**, *78*, 172–174; (b) Grassert, I.; Schinkowski, K.; Vollhardt, D.; Oehme, G. *Chirality* **1998**, *10*, 754–759.

10. Bodanski, M.; Bodanski, A. The Practice of Peptide Synthesis. In *Reaction and Structure Concepts in Organic Chemistry*; Springer: Berlin, 1984, and references cited therein.

11. (a) Kobayashi, M.; Ohno, M. *J. Org. Chem.* **1990**, *55*, 1169–1177; (b) Shiozaki, M.; Arai, M. *J. Org. Chem.* **1989**, *54*, 3754–3755; (c) Kikugawa, Y. *J. Org. Chem.* **1994**, *59*, 929–931.

12. Gouterman, M. In *The Porphyrins*; Dolphin, D., Ed.; Academic: New York, 1978; Vol. 3. Chapter 1.

13. For some examples of aggregation of porphyrin derivatives in aqueous solutions see: (a) Pasternack, R. F.; Huber, P. R.; Boid, P.; Engasser, G.; Francesconi, L.; Gibbs, E.; Fasella, P.; Cerio Venturo, G.; deC. Hinds, L. *J. Am. Chem. Soc.* **1972**, *94*, 4511–4517; (b) Guilard, R.; Senglet, N.; Liu, Y. H.; Sazou, D.; Findsen, E.; Faure, D.; Des Curieres, T.; Kadish, K. M. *Inorg. Chem.* **1991**, *30*, 1898–1905; (c) Schenning, A. P. H. J.; Feiters, M. C.; Nolte, R. J. M. *Tetrahedron Lett.* **1993**, *34*, 7077–7078; (d) Kano, K.; Minamizono, H.; Kitae, T.; Negi, S. *J. Phys. Chem. A* **1997**, *101*, 6118–6124; (e) Ribó, J. M.; Bofill, J. M.; Crusats, J.; Rubires, R. *Chem. Eur. J.* **2001**, *7*, 2733–2737.

14. The cmc of **SDS** is 8.2×10^{-3} M. See, for example, (a) Fendler, J. H.; Fendler, E. J. *Catalysis in Micellar and Macromolecular Systems*; Academic: New York, 1975; (b) The cmc of **L-SDP** has been reported to be 3.0×10^{-3} M (see Ref. 13b). We found, by means of various experimental techniques, a value of 1.0×10^{-2} M, which has been consistently used throughout the work.

15. It has been reported that the inclusion of porphyrin derivatives in **SDS** micelle occurs with significative degree of aggregation. See, for example: Monsú Scolaro, L.; Donato, C.; Castriciano, M.; Romeo, A.; Romeo, R. *Inorg. Chim. Acta* **2000**, *300–302*, 978–986.

16. For a recent survey on Induced Circular Dichroism in micellar systems see: Allenmark, S. *Chirality* **2003**, *15*, 409–422, and references cited therein.

17. The presence of a strong hypochromic effect along with the presence of coupled CD bands are usually taken as an evidence for the formation of porphyrin chiral aggregates. See for example: Fuhrhop, J.-H.; Demoulin, C.; Boettcher, C.; Köning, J.; Siggel, U. *J. Am. Chem. Soc.* **1992**, *114*, 4159–4165.

18. (a) Blatt, E.; Sawyer, W. H. *Biochim. Biophys. Acta* **1985**, *822*, 43–62; (b) van Esch, J. H.; Feiters, M. C.; Peters, A. M.; Nolte, J. M. *J. Phys. Chem.* **1994**, *98*, 5541–5551; (c) Steiner, R. F. In *Topics in Fluorescence Spectroscopy Vol. 2: Principles*; Lakowicz, J. R., Ed.; Plenum: New York, 1991, Chapter 1; (d) Eftink, M. R. *Biophysical and Biochemical Aspects of Fluorescence Spectroscopy*; Plenum: New York, 1987.

19. In previous papers, the notation *trans*- or *cis*-epoxides, has been used, referring to the relative stereochemistry of 1-methylene and the 4-isopropenyl substituents. See, for example, Battioni, P.; Renaud, J. P.; Bartoli, J. F.; Reina-Artiles, M.; Fort, M.; Mansuy, D. *J. Am. Chem. Soc.* **1988**, *110*, 8462–8470. We prefer to use the notation *syn* and *anti* referring to the relative stereochemistry of the 1,2-epoxides and the 4-isopropenyl group.

20. Grassert, I.; Schinkowski, K.; Vollhardt, D.; Oehme, G. *Chirality* **1998**, *10*, 754–759.

21. The extent of chiral induction is well known to largely depend on the steric hindrance at the metal centre. For recent discussions on this important aspect of chiral metalloporphyrin-based catalysts see: (a) Gross, Z.; Ini, S. *J. Org. Chem.* **1997**, *62*, 5514–5521; (b) Tagliatesta, P.; Bernini, R.; Crestini, C.; Monti, D.; Boschi, T.; Mincione, E.; Saladino, R. *J. Org. Chem.* **1999**, *64*, 5361–5365; (c) Reginato, G.; Di Bari, L.; Salvadori, P.; Guilard, R. *Eur. J. Org. Chem.* **2000**, 1165–1171; (d) Boitrel, B.; Bavex-Chambenoît, V.; Richard, P. *Eur. J. Inorg. Chem.* **2002**, 1666–1672.

22. (a) Belogi, G.; Croce, M.; Mancini, G. *Langmuir* **1997**, *13*, 2903–2904; (b) Borocci, S.; Erba, M.; Mancini, G.; Scipioni, A. *Langmuir* **1998**, *14*, 1960–1962; (c) Bella, J.; Borocci, S.; Mancini, G. *Langmuir* **1999**, *15*, 8025–8031; (d) Borocci, S.; Ceccacci, F.; Galantini, L.; Mancini, G.; Monti, D.; Scipioni, A.; Venanzi, M. *Chirality* **2003**, *15*,

441–447; (e) Andreani, R.; Bombelli, C.; Borocci, S.; Lah, J.; Mancini, G.; Mencarelli, P.; Vesnaver, G.; Villani, C. *Tetrahedron: Asymmetry* **2004**, *15*, 987–994; For a recent example of induced chiral discrimination in achiral **SDS** micelle see: (f) Yamada, K.-. I.; Kobori, Y.; Nakagawa, H. *Chem. Commun.* **2000**, 97–98.

23. (a) Geier, G. R., III; Sasaki, T. *Tetrahedron Lett.* **1997**, *38*, 3821–3824; (b) Tamiaki, H.; Onishi, M. *Tetrahedron: Asymmetry* **1999**, *10*, 1029–1032; (c) Tamiaki, H.; Nomura, K.; Muruyama, K. *Bull. Chem. Soc. Jpn.* **1993**, *66*, 3062–3068; (d) Tamiaki, H.; Suzuki, S.; Muruyama, K. *Bull. Chem. Soc. Jpn.* **1993**, *66*, 2633–2637; (e) Hyslop, A. G.; Kellett, M. A.; Iovine, P. R.; Therien, M. J. *J. Am. Chem. Soc.* **1998**, *120*, 12676–12677.

24. (a) Sasaki, T.; Kaiser, E. T. *J. Am. Chem. Soc.* **1989**, *111*, 380–381; (b) Sasaki, T.; Kaiser, E. T. *Biopolymers* **1990**, *29*, 79–88; (c) Lombardi, A.; Nastri, F.; Pavone, V. *Chem. Rev.* **2001**, *101*, 3165–3189; (d) Nastri, F.; Lombardi, A.; D'Andrea, L.; Sanseverino, M.; Miglio, O.; Pavone, V. *Biopolymers* **1998**, *47*, 5–22; (e) Nastri, F.; Lombardi, A.; Morelli, G.; Maglio, O.; D'Auria, G.; Pedone, C.; Pavone, V. *Chem. Eur. J.* **1997**, *3*, 340–349.

25. Robertson, D. E.; Faris, R. S.; Moser, C. H.; Urbauer, J. L.; Mulholland, S. E.; Pidikiti, R.; Lear, J. D.; Wand, A. J.; DeGrado, W. F.; Dutton, P. L. *Nature* **1994**, *368*, 425–434.

26. Perrin, D. D.; Armarego, W. L. F.; Perrin, D. E. *Purification of Laboratory Chemicals*, 2nd ed.; Pergamon: Oxford, 1980.